



LUND UNIVERSITY

Modeling the forest phosphorus nutrition in a southwestern Swedish forest site

Yu, Lin; Zanchi, Giuliana; Akselsson, Cecilia; Wallander, Håkan; Belyazid, Salim

Published in:
Ecological Modelling

DOI:
[10.1016/j.ecolmodel.2017.12.018](https://doi.org/10.1016/j.ecolmodel.2017.12.018)

2018

Document Version:
Peer reviewed version (aka post-print)

[Link to publication](#)

Citation for published version (APA):
Yu, L., Zanchi, G., Akselsson, C., Wallander, H., & Belyazid, S. (2018). Modeling the forest phosphorus nutrition in a southwestern Swedish forest site. *Ecological Modelling*, 369, 88-100.
<https://doi.org/10.1016/j.ecolmodel.2017.12.018>

Total number of authors:
5

Creative Commons License:
CC BY-NC-ND

General rights

Unless other specific re-use rights are stated the following general rights apply:
Copyright and moral rights for the publications made accessible in the public portal are retained by the authors and/or other copyright owners and it is a condition of accessing publications that users recognise and abide by the legal requirements associated with these rights.

- Users may download and print one copy of any publication from the public portal for the purpose of private study or research.
- You may not further distribute the material or use it for any profit-making activity or commercial gain
- You may freely distribute the URL identifying the publication in the public portal

Read more about Creative commons licenses: <https://creativecommons.org/licenses/>

Take down policy

If you believe that this document breaches copyright please contact us providing details, and we will remove access to the work immediately and investigate your claim.

LUND UNIVERSITY

PO Box 117
221 00 Lund
+46 46-222 00 00

Modeling the forest phosphorus nutrition in a southwestern Swedish forest site

Lin Yu^{a,*}, Giuliana Zanchi^b, Cecilia Akselsson^b, Håkan Wallander^c, and Salim Belyazid^d

^a Centre for Environmental and Climate Research, Lund University, Sölvegatan 37, SE-223 62 Lund, Sweden.

^b Department of Physical Geography and Ecosystem Science, Lund University, Sölvegatan 12, SE-223 62 Lund, Sweden.

^c Department of Biology, Lund University, Sölvegatan 37, SE-223 62 Lund, Sweden.

^d Department of Physical Geography, Stockholm University, Svante Arrhenius väg 8, SE-114 18 Stockholm, Sweden.

Abstract

In this study, a phosphorus (P) module containing the biogeochemical P cycle has been developed and integrated into the forest ecosystem model ForSAFE. The model was able to adequately reproduce the measured soil water chemistry, tree biomass (wood and foliage), and the biomass nutrient concentrations at a spruce site in southern Sweden. Both model and measurements indicated that the site showed signs of P limitation at the time of the study, but the model predicted that it may return to an N-limited state in the future if N deposition declines strongly. It is implied by the model that at present time, the plant takes up $0.50 \text{ g P m}^{-2} \text{ y}^{-1}$, of which 80% comes from mineralization and the remainder comes from net inputs, i.e. deposition and weathering. The sorption/desorption equilibrium of P contributed marginally to the supply of bioavailable P, but acted as a buffer, particularly during disturbances.

Keywords:

forest nutrition, phosphorus cycle, nitrogen cycle, ForSAFE, dynamic ecosystem model

* Corresponding author. Current email and address: lyu@bgc-jena.mpg.de, Max Planck Institute for Biogeochemistry, Hans-Knoell-Str. 10, 07745 Jena, Germany
E-mail addresses: giuliana.zanchi@nateko.lu.se (G. Zanchi), cecilia.akselsson@nateko.lu.se (C. Akselsson), hakan.wallander@biol.lu.se (H. Wallander), salim.belyazid@natgeo.su.se (S. Belyazid).

1 Introduction

Forests are among the most important ecosystems on the planet, providing and regulating multiple important services such as timber production, biodiversity conservation, carbon (C) sequestration, bioenergy supply and potable water supply (Nelson et al. 2011, COM 2005). Nitrogen (N) is often reported to limit growth in northern forest ecosystems (Tamm 1991; Jonard et al. 2015). The increase in atmospheric N deposition due to anthropogenic activities has shifted forest ecosystems from being N-limited towards being N-saturated (Aber et al. 1989; Aber et al. 1998), causing N leaching in some forest ecosystems (Gundersen et al. 2006; Kreutzer et al. 2009; Yu et al. 2016). An increased nitrogen pool in the forest can affect other nutrient pools and thereby forest nutrition. It can compromise the availability of base cations by depleting soil base cations through N leaching, which causes acidification and eutrophication (Driscoll et al. 2003; Eriksson et al. 1992; Likens et al. 1996). Another effect of increased N status is a stimulated forest growth (Reich et al. 2006; Ciais et al. 2013), leading to the limitation of other nutrients such as phosphorus (P) (Aber et al. 1989; Akselsson et al. 2008). A switch from N limitation to P limitation over recent decades has been found in many forest studies and experimental studies in Europe (Braun et al. 2010; Jonard et al. 2015; Talkner et al. 2015; Flückiger & Braun 1999) and North America (Crowley et al. 2012; Tessier & Raynal 2003; Gress et al. 2007). Such a transition, from N limitation to P limitation, is not commonly detected in Swedish forests (Ingerslev et al. 2001; Högberg et al. 2006) due to the generally relatively low atmospheric N deposition in Sweden (Simpson et al. 2011). However, in southwestern Sweden, where current and historical N deposition is highest (Akselsson et al. 2010), it is suspected that P limitation might already occur (Rosengren-Brinck & Nihlgård 1995; Akselsson et al. 2008).

Forest P limitation has long been evaluated by the needle N/P ratio (Linder 1995; Rosengren-Brinck & Nihlgård 1995; Mellert & Göttlein 2012; Jonard et al. 2015; Braun et al. 2010), partly because foliar nutrient concentrations and ratios are well-established indicators of nutrient limitation in forest trees (Mellert & Ewald 2014; Jonard et al. 2015). Particularly because P nutrition in forests is more challenging to evaluate than other nutrients, due to the high uncertainties in quantifying the biogeochemical P processes (Frossard et al. 2011; Shen et al. 2011; Fox et al. 2011; Jones & Oburger 2011), and measuring the soil P availability (Shen et al. 2011; Hinsinger 2001). Due to the high uncertainties in P processes measurement, the forest P cycle has not been much quantitatively investigated in field studies (Yanai 1992; Yanai 1998; Jonard et al. 2009), nor has it been soundly evaluated in modeling studies (Jonard et al. 2010; Achat et al. 2009; Wang et al. 2010; Yang et al. 2014; Müller & Bünemann 2014). These highly uncertain P processes include atmospheric deposition (Newman 1995; Tipping et al. 2014), weathering (Newman 1995; Smits et al. 2012), sorption/desorption (McGechan & Lewis 2002; Frossard et al. 2011), mineralization (Bünemann 2015), and rhizosphere processes (Hinsinger 2001; Hinsinger et al. 2011). Nevertheless, forest P cycle and its impacts on other cycles (e.g. C and N) are much less investigated in modeling studies simply due to the absence of P cycle in most forest/terrestrial ecosystem models (Fontes et al. 2010; Flato et al. 2013).

In this paper, we first implemented a P module, which contains the biogeochemical processes of the full P cycle, into the integrated dynamic forest model, ForSAFE. We then tested the model at a southwestern Swedish forest site, which is at high risk of P limitation. The aims of this study were: 1) to evaluate the forest nutrition (N and P) at the study site, 2) to quantify the forest P cycle, especially the biogeochemical P processes, from a modeling perspective.

2 Methods

2.1 The ForSAFE model

ForSAFE is a mechanistic biogeochemical model of the forest ecosystem and was designed to simulate the dynamic responses of the forest ecosystem to environmental changes (Zanchi et al. 2014; Yu et al. 2016). The model aggregates independent processes—chemical, physical, and physiological—based on empirical evidence (Belyazid 2006; Wallman et al. 2005). These independent but mutually interacting processes bring together three basic material and energy cycles to form a single integrated model: 1) the biological cycle, representing the processes involved in tree growth; 2) the biochemical cycle, including uptake, litter decomposition, and soil nutrient dynamics; and 3) the geochemical cycle, including atmospheric deposition and weathering processes (Fig. 1).

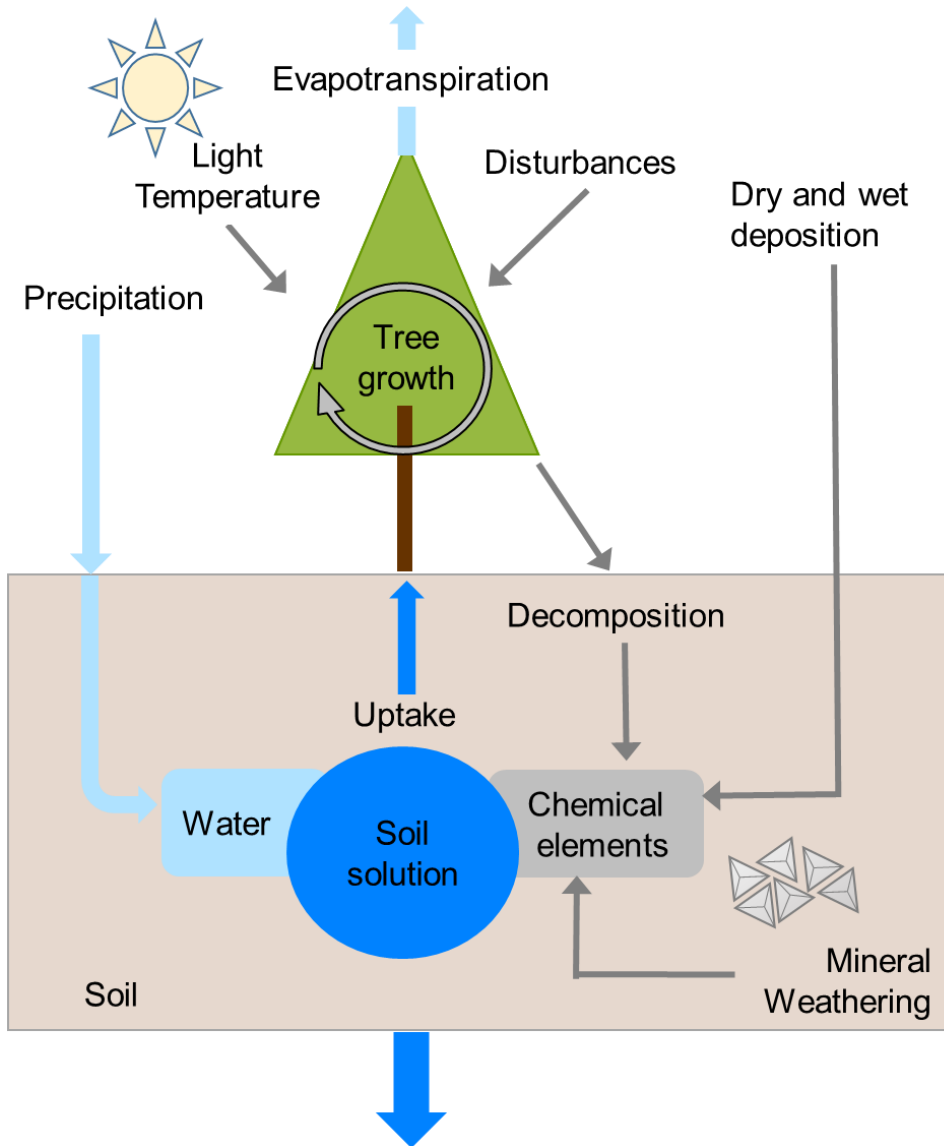


Figure 1. The ForSAFE model. Climate input parameters (radiation, temperature, and precipitation) drive vegetation growth. Nutrient and water availability constrain growth to the actual biomass growth and nutrient accumulation (Adapted from Zanchi et al. 2014).

ForSAFE consists of four modules based on the concepts of four established models: the tree growth model PnET (Aber & Federer 1992), the soil chemistry model SAFE (Alveteg 1998), the decomposition model Decom (Wallman et al. 2006; Walse et al. 1998), and the hydrology model PULSE (Lindström & Gardelin 1992). The elements simulated in the soil chemistry module are nitrates (NO_3^-), ammonium (NH_4^+), base cations (calcium ions [Ca^{2+}], magnesium ions [Mg^{2+}], potassium ions [K^+], sodium ions (Na^+), aluminum ions (Al^{3+}), sulfates (SO_4^{2-}), chloride ions (Cl^-), hydrogen ions (H^+) and dissolved organic carbon (DOC). Among these, only N and base cations are treated as macronutrients for trees and are therefore modeled in the tree growth and decomposition modules. The hydrology module models the soil hydrology process and traces the dynamics of soil water flows and soil water contents.

2.2 Inclusion of the phosphorus cycle

In order to better represent the biogeochemical P processes, several changes were made prior to the inclusion of the P cycle. They are outlined below (Detailed description in Appendix A).

- The soil hydrology process was modified based on the new ForSAFE hydrology module developed by Zanchi et al. (2016) to better represent the soil water content and soil water flow, which in turn regulate the C and nutrient cycles.
- The decomposition process was complemented with concepts from three existing models (Schimel & Weintraub 2003; Moorhead & Sinsabaugh 2006; Parton et al. 1988), and a microbial component was explicitly added to regulate the C and nutrient fluxes in the decomposition process.
- The tree growth process was modified by changes in the tree structure, plant uptake, and C and nutrient allocations in order to simulate realistic plant nutrient uptake and nutrient contents, particularly for those of P.
- The length of the time step was reduced from monthly to daily to better simulate the hydrology process, the microbial dynamics and the P cycle, particularly the sorption/desorption equilibrium.

The biogeochemical P processes that were taken account in the model are deposition, weathering, sorption and desorption, occlusion and mineralization, which includes both biological mineralization and biochemical mineralization (Fig. 2). The external inputs of P to the forest ecosystem are atmospheric deposition and mineral weathering. Deposition is treated as an input in the model, and weathering is simulated by the soil chemistry module. The outputs of P from the forest ecosystem are through harvesting and leaching and are simulated in the same way as N (Wallman et al. 2005). The P processes in the tree growth and decomposition modules are also simulated in the same way as those of N, except that biochemical mineralization of P is included (P mineralization catalyzed by enzymes, without releasing CO_2 , McGill & Cole 1981; Oberson & Joner 2005). The P processes in the soil chemistry module are weathering, sorption/desorption, and occlusion. The soil inorganic P is stored in soil solution as dissolved inorganic P, in the soil matrix as sorbed inorganic P and occluded inorganic P, and in soil minerals as mineral P (Fig. 2). All the inorganic P in ForSAFE is considered to be orthophosphate (PO_4^{3-}), but the distinctions between different forms of orthophosphate (H_2PO_4^- , HPO_4^{2-} and PO_4^{3-}) are not simulated in the model. The dissolved inorganic P concentration is determined by all the processes that exert a direct effect on it (fertilization, deposition,

124 weathering, plant uptake, immobilization/mineralization and sorption/desorption). Further details
125 of the processes descriptions can be found in Appendix A4.

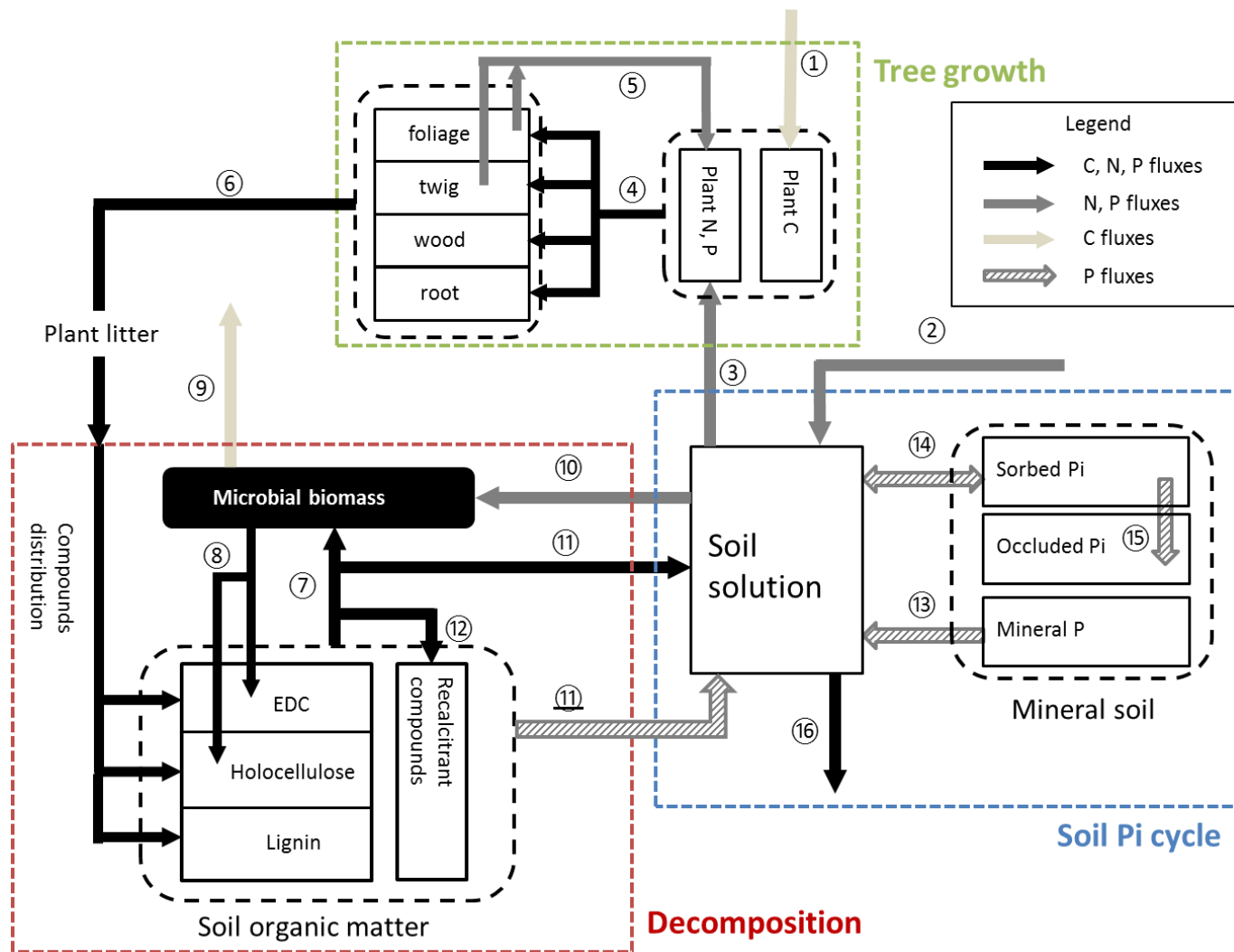


Figure 2. Major carbon and nutrient processes in ForSAFE: ① photosynthesis, ② deposition, ③ plant nutrient uptake, ④ allocation, ⑤ retranslocation, ⑥ litter fall, ⑦ microbial assimilation, ⑧ microbial decay and overflow metabolism, ⑨ microbial respiration, ⑩ immobilization, ⑪ biological mineralization and overflow metabolism mineralization, ⑫ humification, ⑬ P weathering, ⑭ P sorption/desorption, ⑮ P occlusion, ⑯ nutrient leaching (percolation and surface flow). EDC: easily decomposable carbon; Pi: inorganic phosphorus.

2.3 Site description

Klintaskogen is a Norway spruce (*Picea abies* Karst) forest site in southwest Sweden. The average annual precipitation is 780 mm and the average annual temperature is 7.2 °C (annual average between 1961 and 2010). It is a managed forest that was planted on juniperous grassland in the 19th century. The latest clear-cut occurred in 1957, and the site was replanted with Norway spruce. The site suffered from the wind storm *Lothar* in December 1999 and another wind storm *Gudrun* in January 2005, both of which caused windthrow of the trees at the site (15% and 5%, respectively).

The site has a very thin forest floor (3.5 cm) with 48% organic matter content. The top 50cm of the mineral soil is sandy and acidic, featured with very low base saturation and high occupation of Al^{3+} in the exchangeable sites. The soil is categorized as dystric podzols.

The measurement values of forest inventory data and soil chemistry data for the model evaluation are presented in Yu et al. (2016). The soil inputs and model implementation are given in the supplementary material.

2.4 Sensitivity analysis and model calibration

The parameters used in ForSAFE include parameters of tree growth, decomposition, mineralization, and P sorption/desorption (Given in supplementary material). Compared to the previous version of ForSAFE, the decomposition and mineralization parameters have been changed as a result of changes in model concepts, such as the incorporation of processes regulated by microbial activity. A regression-based sensitivity analysis was carried out to estimate the impact of the modified parameters on selected outputs and to calibrate the model. Twenty-two parameters regulating decomposition and tree growth were allowed to vary independently and randomly within given ranges (Supplementary material, Table S.2), generating a total of 1000 parameter sets. The standardized regression coefficients (SRCs) (Cariboni et al. 2007; Santner et al. 2003) of each parameter on the selected outputs—the average rates of N leaching, N mineralization, P weathering, P desorption, biological P mineralization and biochemical P mineralization during the period 1980–2015—were calculated.

The performance of the model was evaluated against the measured wood biomass, needle N and needle P concentrations and needle N/P ratios, the measured soil water chemistry data at a depth of 50 cm, and the soil organic content (C, N, and P) of the forest floor. The best fit to measured data was chosen from the 1000 parameter sets in the sensitivity analysis, firstly by comparing the linear relationships between measurements and the results of the model, and secondly by visually inspecting the similarities between the curves obtained from measurements and the model.

All statistical analysis was carried out with RStudio software (R Core Team, 2013) and the SRCs were calculated using the package QuantPsync (Fletcher 2015).

3 Results

3.1 Model evaluation

The model overestimated the wood biomass by 17% and underestimated the foliage biomass by 13%, but the modeled trends for the change in wood biomass and leaf biomass agreed well with the measurements (Fig. 3). The modeled needle N concentrations were about 5% lower than the forest inventory data. Although less noticeable, the model still captured the decrease in needle N concentration after 2000. The modeled needle P concentrations were within the range of the forest inventory data, but the model did not capture the change in needle P concentration due to storm disturbances.

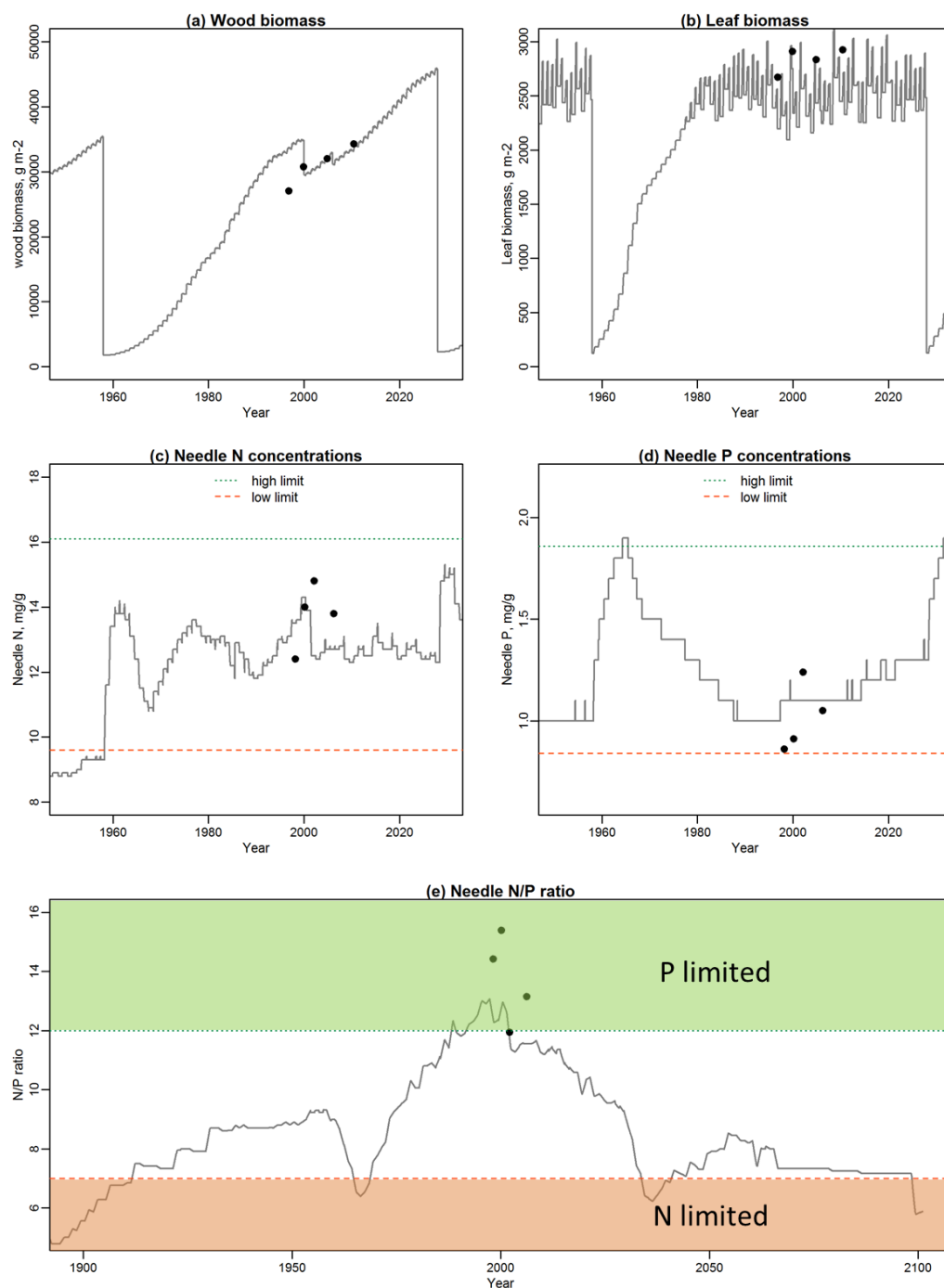


Figure 3. Comparison of modeled and measured wood biomass, and needle N and P concentrations during 1950–2010 (subplots (a) to (d)), and modeled and measured needle N/P ratio during 1900–2100 (subplot (e)). The black dots are calculated from measurements. Subplots (a) to (d): the low limits (dashed lines) and high limits (dotted lines) for needle N and P concentrations are based on the 5 and 95 percentile values given in ICP (International Co-operative Programme on Assessment and Monitoring of Air Pollution Effects on Forests) report (Fischer & Lortenz 2011); Subplot (e): the lines/areas of N/P ratios for N and P limitations are based on estimates by Mellert and Göttelein (2012)’s review, in which new threshold values and ratios for N and P for Norway spruce are derived from a literature compilation.

184 The modeled needle N/P ratio generally increased from 1900 until it reached a peak around
185 2000, after which it decreased (Fig. 3). Although the occurrence of the P limitation was captured
186 by the model, the needle N/P ratio was considerably underestimated around 2000, indicating that
187 forest P nutrition might be worse than the model prediction.

188 The simulated soil water chemistry generally agreed with the measurements available in 1997–
189 2009, although there was a major discrepancy in the modeling of base cations (Fig. 4). The
190 model captured the temporal trends and the ranges of the measurements for the majority of the
191 chemicals in soil water, but the modeled yearly mean values were mostly lower than the
192 measurements. We observed that N was leached out over the whole monitoring period, and N
193 leaching increased after 2000 following the storms. The model results confirmed that N was
194 leached out continuously, and the storm disturbances caused a peak in N concentration after
195 2000. Although the linear correlation between modeled pH and measured pH seems good, the
196 model actually overestimated the soil water pH by about 0.3 units and failed to capture the
197 temporal trend of pH.

198 C, N and P contents in soil organic matter (SOM) were only measured in 2010, and the model
199 predicted the SOM C and N contents very well, but clearly overestimated the SOM P content
200 (Fig. S1). As only one measured value was available, it was not possible to evaluate the
201 predicted change in SOM C, N and P contents in this study.

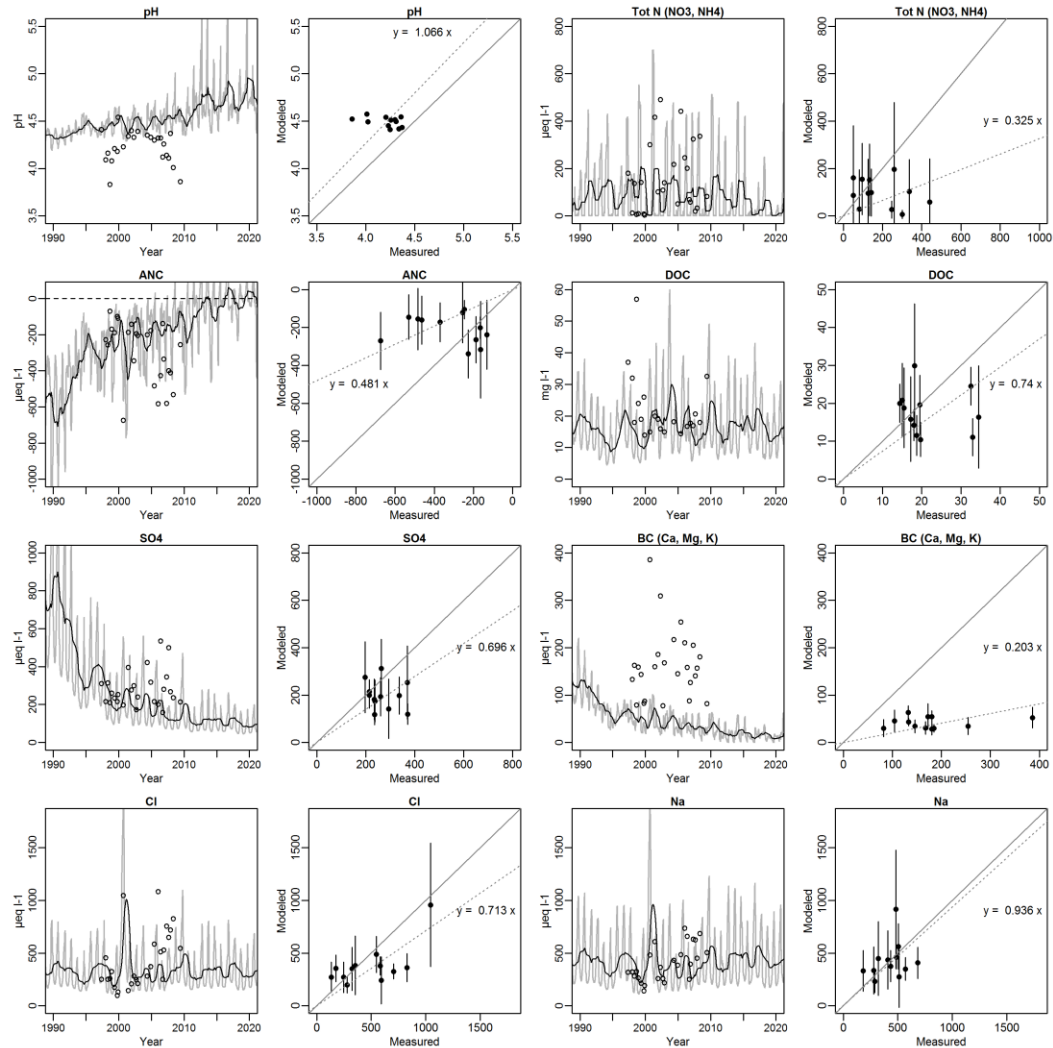


Figure 4. Comparison of modeled and measured soil water chemistry data. The gray curves show the modeled monthly values and the black lines the moving averages (365-day periods) of these values. ANC denotes acid neutralizing capacity, ○—measurements, and ●—yearly mean values. The dotted line and its slope give an indication of the discrepancy between the modeled values and measured data. The soil water was collected at a depth of 50 cm.

3.2 The long-term forest N and P budgets

In the model, it is assumed that N enters the forest ecosystem only through deposition and that it can be stored in tree biomass, in SOM, or leach out (Table 1). Over the simulation period, 30% of the N inputs accumulated in the tree biomass, 26% was leached out, and 44% was accumulated in the SOM. The forest receives one-third of its P input from deposition and two-thirds from weathering. P can be stored in the soil matrix, tree biomass or SOM, and a small amount of it leaches out (Table 1). Over the whole simulation period, 44% of the P input accumulated in the tree biomass, 55% accumulated in the SOM and 1% was leached out. The masses of N and P given by the model are well conserved over the 300-years period (109 938 time steps), with total error level of 10^{-5} g m⁻² for N and 10^{-13} g m⁻² for P. From the forest ecosystem perspective, N and P leave the forest through harvesting and leaching, thus their budgets follow ‘deposition + weathering + desorption = harvesting + leaching + accumulation in

trees + accumulation in SOM^a. The model showed that Klintaskogen forest accumulated both N (160.20 g m⁻²) and P (11.80 g m⁻²) in SOM over the simulation period.

Table 1. Cumulative sinks and sources of N and P at Klintaskogen during the period 1800–2100^a

	Sources (g m ⁻²)			Sinks (g m ⁻²)			
	Deposition	Weathering	Desorption	Acc. in trees ^b	Harvest	Acc. in SOM	Leaching
N	382.09	0	0	-5.68	121.09	165.86	100.82
P	8	14.84	0.13	-0.9	10.96	12.69	0.22

^aSources refers to the inputs to the forest; Sinks refers to both outputs and accumulation in the forest. Sources = Sinks in every time step and over the whole simulation period.

^bAcc. denotes Accumulation; Acc. in tree biomass is the change in the plant pool, where negative values indicate net decreases.

3.3 Dissolved inorganic N and P fluxes in soil water

The inputs of N and P were not sufficient to support the plant uptake in the model simulation, thus the internal processes—biological mineralization, biochemical mineralization, and desorption—played important roles in supplying nutrients for uptake from the soil water (Fig. 5). Over the period of forest rotation (1900–2100), the soil water received a total of 1015 g N m⁻² (biological mineralization 707 g N m⁻²; deposition 308 g N m⁻²), of which 9% was lost through leaching, and the remainder was taken up by plants (91%, in total 922 g N m⁻²). In contrast, the P inputs (deposition and weathering) supplied only about 16% of the total influxes to soil water, while biological and biochemical processes provided 41% and 43%, respectively. Most of the dissolved inorganic P in soil water was taken up by plants (99.3%, in total 104.8 g P m⁻²).

As can be seen in Fig. 5(a), despite a short period of N leaching after thinning in 1912, very little N leached out during the first forest rotation (before 1957). However, after the clear-cut in 1957, N leached out continuously as a consequence of disturbances, both natural (storms) and anthropogenic (thinnings, clear cuts). In the future (2027–2097), the model predicts lower N leaching after disturbances. The N mineralization rate generally followed the pattern of plant N uptake, and periods of high fluxes were predicted after each clear-cut and thinning.

P inputs (deposition + weathering) did not vary significantly over the forest rotation period, whereas other fluxes (biological mineralization, biochemical mineralization and desorption) fluctuated over the whole simulation period, especially after disturbances, such as clear-cuts, thinning and storms (Fig. 5(b)). It can be seen that after each clear-cut, the release of dissolved inorganic P from the soil was increased due to biological mineralization and biochemical mineralization; most of the released P was taken up by plants or sorbed by the soil matrix. Although the desorption rate fluctuated considerably over the simulation period, the total P desorption during 1900–2100 was only -0.4 g m⁻². The total biological P mineralization was 43.0 g m⁻² and the total biochemical P mineralization was 45.9 g m⁻².

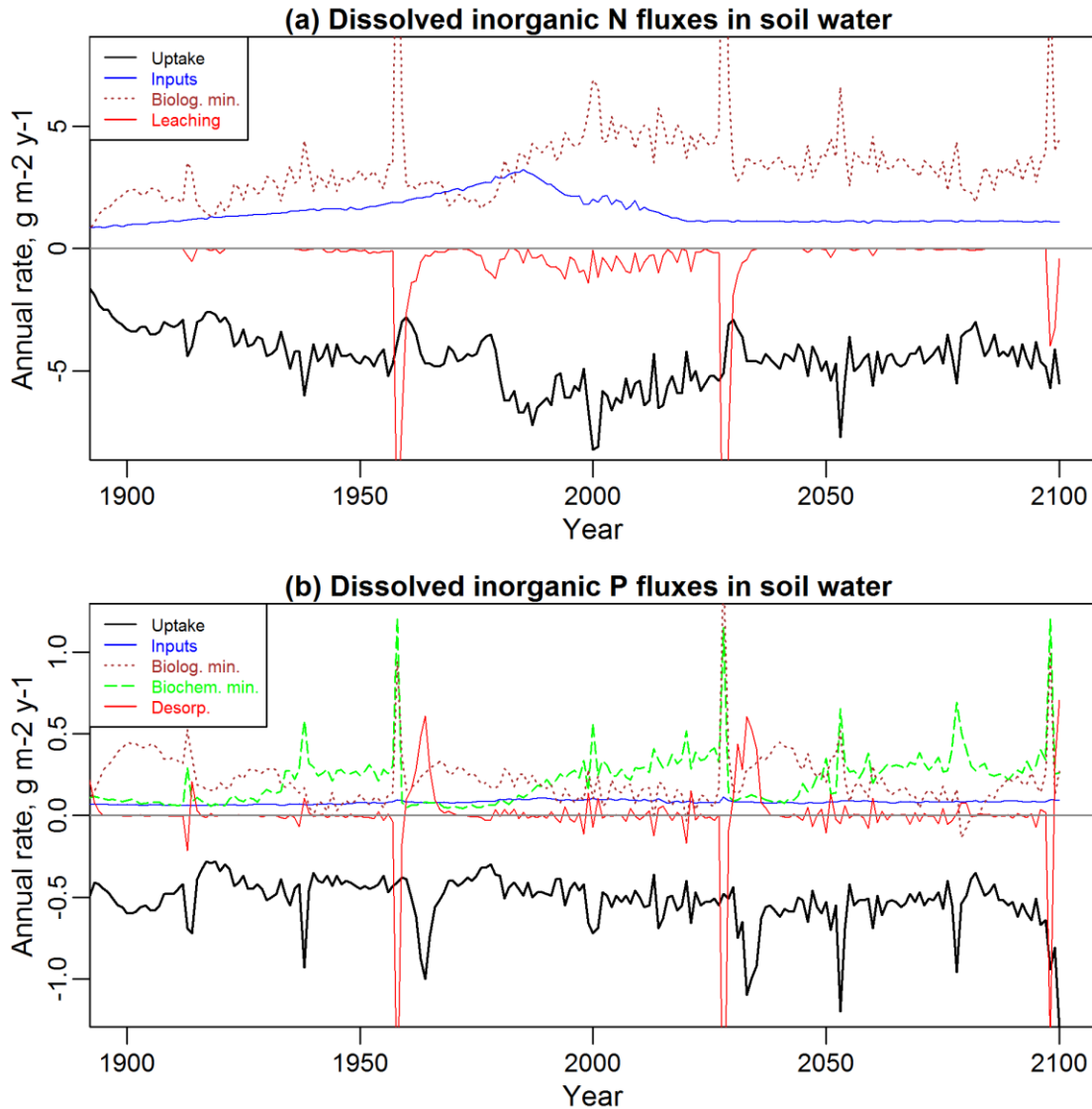


Figure 5. Modeled dynamics of dissolved inorganic N fluxes (a) and P fluxes (b) in soil water over the period 1900–2100. Biolog. min.: net rate of biological mineralization; Biochem. min.: rate of biochemical mineralization; Desorp.: desorption. In (a), plant N uptake + N leaching = N inputs + Biolog. N min., where N inputs include only deposition. In (b), plant P uptake = P inputs + Biolog. P min. + Biochem. P min. + Desorp. P, where P inputs include deposition and weathering. P leaching was ignored in (b) due to its low amount.

3.4 Sensitivity analysis

As shown in Table 2, the weathering of P is the least sensitive to changes in the selected parameters, showing less than 5% difference between the 10th percentile value and 90th percentile value. N leaching seems to be most sensitive to changes in the selected parameters, showing a difference of two orders of magnitude between the 10th percentile value and the 90th percentile value. For the other the parameters studied (N mineralization, biological P mineralization, biochemical P mineralization and P desorption), the variances between the 10th percentile value and the 90th percentile value are within one order of magnitude.

Table 2. The 10th percentile values, median values and 90th percentile values of the selected outputs in the sensitivity analysis. The values are the average rates (g m⁻² y⁻¹) between 1980 and 2015.

Selected outputs	10 th percentile	Median	90 th percentile
N leaching	0.015	0.63	1.028
N mineralization	3.09	5.14	6.10
Biolog. P min.^a	-0.059	0.26	0.56
Biochem. P min.^b	0.053	0.20	0.55
P min. Total	0.23	0.49	0.79
P weathering	0.070	0.071	0.072
P desorption	-0.0016	-0.00023	0.0066

^aBiological P mineralization

^bBiochemical P mineralization

In general, the adjusted value of R² of the first-order regressions between the selected parameters and outputs are very low (Supplementary material, Table S.3), indicating that the model is highly non-linear and that a single parameter can only explain a very small fraction of the variance in the output. However, the fraction of humification during DOC decomposition seems to have a much stronger impact on the selected outputs than other parameters.

4 Discussions

4.1 Forest nutrition at the study site

Swedish forests are mostly limited by N due to low N deposition (Akselsson et al. 2007; Akselsson et al. 2008). Previous forest studies in Sweden have shown that Swedish forests usually have either relatively high needle P concentrations (Vestin et al. 2013; Rothpfeffer & Karlton 2007) or low needle N/P ratios due to very low needle N concentrations (Bauer et al. 1997; Anonymous 2003). However, low needle P concentrations or high needle N/P ratios (>10) have been reported in southern Sweden, suggesting P limitation (Rosengren-Brinck & Nihlgård 1995; Majdi & Rosengren-Brinck 1994; Ericsson et al. 1995; Wallander & Thelin 2008) or co-limitation by N and P (Rosengren-Brinck & Nihlgård 1995). The forest inventory data from the present study show that Klintaskogen had very low needle P concentrations and very high needle N/P ratios before the storm disturbance. Although the needle P concentrations seem to increase somehow after the storms, the needle N/P ratios still remained high (Fig. 3). The observed N leaching in soil water both before and after the storms also indicates that the site is approaching, or is already at N saturation. Based on the above, we believe that Klintaskogen is already P-limited today.

The model simulation confirms the P limitation at present day with the highest foliar N/P ratio (Fig. 3), the highest N leaching (Fig. 4&5) and the lowest SOM C/N ratio (Fig. S1) of the entire simulation period. It also indicates that Klintaskogen gradually changed from an N-limited to a P-limited forest from 1900 to the present time, but will return to being N-limited again in the future (Fig. 3). The simulated forest nutrition, i.e. the needle N, P concentrations, and needle N/P ratios, is majorly determined by the plant uptake of N and P, which are dominated by the mineralization rates. For the modeled N mineralization rate, besides a strong microbial impact (Table 2), our model results show a correlation between N deposition and N mineralization (3:7). In the forest N budget studies of Korhonen et al. (2013) and Kreutzer et al. (2009), similar correlations were found under two different N deposition (7.4 and $45 \text{ kg N ha}^{-1} \text{ y}^{-1}$). This might imply a universal correlation between N inputs (deposition) and N mineralization in the coniferous forest ecosystem. But it needs to be interpreted carefully because the role of biological N fixation is largely unknown in our model and in their studies.

In contrast, the rate of P inputs—deposition and weathering—is relatively stable over the simulation period, as is the plant P uptake rate (Fig. 5). The biological P mineralization varies considerably over the period, but the overall plant P uptake does not change to the same degree (Fig. 5, Table 2). This probably indicates, firstly, that the P inputs do not have as strong regulating effects on the P cycle as the N inputs have on N cycle; and secondly, the biochemical P mineralization and P desorption can somehow compensate for the change in biological P mineralization, thus leading to a more stable plant P uptake rate than N. Above all, the prediction of the needle N/P ratio seems to be most influenced by the changes in N deposition, and we predict that in the future, the forest will be N-limited under the low future N deposition projection we used. However, this speculation holds a high uncertainty due to the highly uncertain future N deposition (Fowler et al. 2013), and the specific site condition we modeled, but we do believe future studies on other forest sites under different N deposition scenarios will enlighten us about the interactions of nutrient cycles in the changing climate.

4.2 The modeled forest P cycle

Over the past 35 years (1980–2015), it was estimated that trees took up $0.50 \text{ g P m}^{-2} \text{ y}^{-1}$, to which biochemical P mineralization ($0.23 \text{ g P m}^{-2} \text{ y}^{-1}$) and biological P mineralization ($0.17 \text{ g P m}^{-2} \text{ y}^{-1}$) contributed 46% and 34% respectively. The remaining 20% consisted of deposition ($0.027 \text{ g P m}^{-2} \text{ y}^{-1}$), weathering ($0.071 \text{ g P m}^{-2} \text{ y}^{-1}$) and desorption ($0.001 \text{ g P m}^{-2} \text{ y}^{-1}$). The plant P uptake rate is difficult to measure *in situ* and is usually estimated by measuring the plant P demand, assuming P equilibrium in the plant (Johnson et al. 2003; Yang & Post 2011). Our modeled plant P uptake rate is in good agreement with the value reported by Johnson et al. (2003) for temperate forests ($0.52 \pm 0.38 \text{ g P m}^{-2} \text{ y}^{-1}$), but is notably higher than the modeled P uptake rate of coniferous evergreen forest by Goll et al. (2012) ($0.20 \text{ g P m}^{-2} \text{ y}^{-1}$). We believe that our predicted P uptake rate is more realistic as the model also reproduced the wood biomass, leaf biomass, and leaf P concentration well.

The model predicts that mineralization is the most important source of plant P uptake, which is in agreement with the findings in many other studies (Jonard et al. 2009; Achat et al. 2010; Yanai 1992; Attiwill & Adams 1993; Cross & Schlesinger 1995). Biochemical mineralization is believed to be an important mechanism immobilizing organic P under P deficiency, and has been widely incorporated into terrestrial ecosystem models (Wang et al. 2007; Jonard et al. 2010; Goll et al. 2012; Yang et al. 2014; Runyan & D’Odorico 2012). Our model results indicate that the biochemical P mineralization fluctuates over the whole simulation period, and responds strongly to disturbances such as clear-cuts and storms, for two main reasons. The first is that we allow the enzyme to cleave P not only from the stable organic matter but also from partially decomposed lignin and holocellulose; and the second is that the microbial biomass increases dramatically after disturbances, thus producing more enzymes, as has been seen *in situ* after logging (Adamczyk et al. 2015). Our modeled biochemical P mineralization rates are thus generally higher than those from other models, and the biological P mineralization rates are lower but are still of the same magnitude comparable to estimates from other studies (e.g. Goll et al. (2012) and Wang et al. (2007)). However, the model evaluation of P mineralization has always been a problem since it is still not yet measurable in field scale. We believe that recent advances in *ex situ* P mineralization measurement (Frossard et al. 2011; Bünemann 2015) could possibly provide better information to constrain the model predictions in future.

Desorption of P is considered an important supplement to plant P uptake, especially in highly weathered soils (e.g. tropical forests, Yang et al. 2014). Our results show that the P sorption/desorption equilibrium plays an important role in regulating plant P uptake, especially after disturbances such as clear-cuts (Fig. 5). But the overall contribution of P desorption to plant P uptake is very small (Tables 1&2), indicating that in a sandy podzol soil, the soil-sorbed P pool acts more as a ‘buffering’ pool rather than a source of P for plant uptake.

Little attention was paid to deposition and weathering in previous P cycle studies, due to the model limitations or a lack of data. The present study clearly shows that deposition and weathering are also important sources for plant P uptake (ca. 20%). From the whole ecosystem’s perspective, the deposition and weathering are even more profound because they are the sole P inputs to the ecosystem. Our predicted P weathering rate is very high compared to a previous Swedish study (Akselsson et al. 2008), thus resulting in a higher accumulation rate of P in the forest (Table 1). We have identified a possible overestimation of weathering rate in the model and will continue to investigate its impact on the P cycle (Martin Erlandsson Lampa, personal communication).

Recent studies on some German spruce forest sites have inferred that forest P cycle strategies could evolve from ‘acquiring system’ to ‘recycling system’ as the soil P availability decreases (Lang et al. 2017). The level of podsolization could be used an important indicator to know the forest ecosystem’s P status—the later stage podsolization is, the more dominant by organic P cycling (recycling system) (Werner et al. 2017). The high Al^{3+} exchangeable sites and low soil C:P ratio (data not shown) at Klintaskogen indicate that the site is still at the early-mediate stage of podsolization. This is also partly confirmed by our model results that weathering is still an important source of plant uptake, and SOM is still able to accumulate organic P over the long term. However, the model capacity to simulate the forest’s P cycling strategy needs to be properly investigated in future.

4.3 Model development and sensitivity analysis

With the incorporation of the full P cycle, the new version of ForSAFE is able to reproduce the observed soil water chemistry and forestry inventory data. One important improvement is that the increased soil water N concentrations after storm disturbance can now be simulated without changing the parameter values regulating the immobilization rate in the model (Yu et al. 2016). We believe that the incorporation of microbial regulation on the decomposition process enables the model to better represent the nutrient dynamics after disturbances. However, a major discrepancy in the modeling of base cation concentrations occurred with the incorporation of microbial processes. It requires future development of base cation cycle in the model.

We are not surprised that each parameter alone had a very small impact on the model outputs (Table S.3) as the model is very complex and highly non-linear. The humification fraction during DOC decomposition has a much greater impact on model outputs than other parameters. It indicates that the dissolved inorganic/organic nutrients associated with DOC are essentially regulating the nutrient cycle in our model, probably because the humification process is the dominant process for SOM formation in the model. We also observed a systematic overestimation of SOM P content in forest floor and a systematic underestimation of SOM C and SOM N content in mineral soils (data not shown). It strongly implies that we should improve the descriptions of biological, chemical, and physical processes in SOM, such as including autotrophic microbial controls and vertical transport processes such as bioturbation and particle fluxes (Ahrens et al. 2015).

The incorporation of P in ForSAFE naturally decreases the simulated productivity of the forest and challenges the existing assumptions regarding C sequestration and allocation in the model. The productivity change was not specifically investigated in this study as other changes might also contribute to it. This must be further studied in the future because it may have a significant impact on the C cycle and related ecosystem services, such as timber production and climate regulation. Nevertheless, the incorporation of P cycle enables us to predict future forest nutrition, to better evaluate the nutrient fluxes in soil water, and to study the organic C and nutrient cycles. Although the evaluation of the model against empirical data is impossible for most of the P processes due to the technical difficulties in measurements, the simulation of the P cycle still provides valuable information on some of the less well-understood processes, such as P weathering, biochemical P mineralization, and P sorption/desorption equilibrium.

5 Conclusions

The ForSAFE model was implemented with a P module containing the biogeochemical P cycle and tested at Klintaskogen forest site. Both the forest inventory data and the model results supported the suspicion that Klintaskogen is already limited by P. The model simulations showed that between 1900 and 2000 the site switched from being N-limited to being P-limited, and in future the site may return to N limitation, however, this prediction is heavily dependent on the low future projection of N deposition. The model showed that at present period, Klintaskogen forest took up $0.50 \text{ g P m}^{-2} \text{ y}^{-1}$, to which biochemical P mineralization ($0.23 \text{ g P m}^{-2} \text{ y}^{-1}$) and biological P mineralization ($0.17 \text{ g P m}^{-2} \text{ y}^{-1}$) together contributed 80%, while deposition, weathering, and desorption constituted the remaining 20%. The importance of P deposition and weathering in forest ecosystems should be highlighted, firstly due to their contributions to plant uptake, and secondly due to the role as the sole inputs to the system. At Klintaskogen, the P sorption/desorption equilibrium contributes very little to plant P uptake in the long term, but it can regulate the plant P uptake rate, especially after disturbances.

With the current model structure and processes, ForSAFE adequately reproduced the measured soil water chemistry, the measured tree biomass and its chemical composition, including the needle N and P concentrations of the study site. Although we are aware of different sources of uncertainties and the study/model limitations, we have moderate confidence in the modeled forest nutrition and forest P cycle. Some of the less well-understood processes that we addressed here, such as P weathering, biochemical P mineralization, and P sorption/desorption equilibrium, should be further investigated in both field and modeling studies.

Acknowledgments

The authors wish to express their gratitude for the financial support granted by the project “Biodiversity and Ecosystem services in a Changing Climate” (BECC). We also thank Gregory van der Heijden, Nicholas Rosenstock, Ann-Mari Fransson, Christian Morel and Pål Axel Olsson for their valuable advice on model development.

References

- Aber, J. et al., 1998. Nitrogen saturation in temperate forest ecosystems - Hypotheses revisited. *Bioscience*, 48(11), pp.921–934.
- Aber, J.D. et al., 1989. Nitrogen saturation in northern forest ecosystems. *BioScience*, 39(6), pp.378–386.
- Aber, J.D. & Federer, C.A., 1992. A generalized, lumped-parameter model of photosynthesis, evaporation and net primary production in temperate and boreal forest ecosystems. *Oecologia*, 92(4), pp.463–474.
- Achat, D.L. et al., 2010. Long-term organic phosphorus mineralization in Spodosols under forests and its relation to carbon and nitrogen mineralization. *Soil Biology and Biochemistry*, 42(9), pp.1479–1490.
- Achat, D.L., Bakker, M.R. & Morel, C., 2009. Process-Based Assessment of Phosphorus Availability in a Low Phosphorus Sorbing Forest Soil using Isotopic Dilution Methods. *Soil Science Society of America Journal*, 73(6), p.2131.
- Adamczyk, B. et al., 2015. Logging residue harvest may decrease enzymatic activity of boreal forest soils. *Soil Biology and Biochemistry*, 82, pp.74–80.
- Ahrens, B. et al., 2015. Contribution of sorption, DOC transport and microbial interactions to the 14C age of a soil organic carbon profile: Insights from a calibrated process model. *Soil Biology and Biochemistry*, 88, pp.390–402.
- Akselsson, C. et al., 2010. Assessing the risk of N leaching from forest soils across a steep N deposition gradient in Sweden. *Environmental pollution*, 158(12), pp.3588–3595.
- Akselsson, C. et al., 2007. Nutrient and carbon budgets in forest soils as decision support in sustainable forest management. *Forest Ecology and Management*, 238(1–3), pp.167–174.
- Akselsson, C. et al., 2008. The influence of N load and harvest intensity on the risk of P limitation in Swedish forest soils. *Science of the Total Environment*, 404(2–3), pp.284–289.
- Alveteg, M., 1998. *Dynamics of Forest Soil Chemistry*. Lund, Sweden: KFS.
- Anonymous, 2003. *Ecocyclic pulp mill – “KAM”. Final report 1996–2002.*, Stockholm.
- Attiwill, P.M. & Adams, M.A., 1993. Nutrient cycling in forests. *New Phytologist*, 124(50), pp.561–582.
- Bauer, G., Schulze, E.D. & Mund, M., 1997. Nutrient contents and concentrations in relation to growth of *Picea abies* and *Fagus sylvatica* along a European transect. *Tree Physiology*, 17(12), pp.777–86.
- Belyazid, S., 2006. *Dynamic modelling of biogeochemical processes in forest ecosystems*. Lund, Sweden: Department of Chemical Engineering, Lund University.
- Berg, B. & McLaugherty, C., 2008. *Plant Litter: Decomposition, Humus Formation, Carbon Sequestration* 2nd ed., Berlin, Heidelberg: Springer Berlin Heidelberg.
- Braun, S. et al., 2010. Does nitrogen deposition increase forest production? The role of phosphorus. *Environmental Pollution*, 158(6), pp.2043–2052.
- Bünemann, E.K., 2015. Soil Biology & Biochemistry Assessment of gross and net mineralization rates of soil organic phosphorus e A review. *Soil Biology and Biochemistry*, 89, pp.82–98.
- Cariboni, J. et al., 2007. The role of sensitivity analysis in ecological modelling. *Ecological Modelling*, 203(1–2), pp.167–182.
- Ciais, P. et al., 2013. Carbon and Other Biogeochemical Cycles. In T. F. Stocker et al., eds. *Climate Change 2013: The Physical Science Basis*. Cambridge, United Kingdom and New York, NY, USA: Cambridge University Press, pp. 465–570.
- Cleveland, C.C. & Liptzin, D., 2007. C:N:P stoichiometry in soil: Is there a “Redfield ratio” for the microbial biomass? *Biogeochemistry*, 85(3), pp.235–252.
- Cross, A.F. & Schlesinger, W.H., 1995. A literature review and evaluation of the Hedley fractionation: Applications to the biogeochemical cycle of soil phosphorus in natural ecosystems. *Geoderma*, 64(3–4), pp.197–214.

- Crowley, K.F. et al., 2012. Do Nutrient Limitation Patterns Shift from Nitrogen Toward Phosphorus with Increasing Nitrogen Deposition Across the Northeastern United States? *Ecosystems*, 15(6), pp.940–957.
- Driscoll, C.T. et al., 2003. Effects of acidic deposition on forest and aquatic ecosystems in New York State. *Environmental Pollution*, 123(3), pp.327–336.
- Ericsson, A. et al., 1995. Concentrations of mineral nutrients and arginine in needles of *Picea abies* trees from different areas in southern Sweden in relation to nitrogen deposition and humus form. *Ecological Bulletins*, 44(44), pp.147–157.
- Eriksson, E., Karlton, E. & Lundmark, J., 1992. Acidification of in Sweden Forest. *Ambio*, 21(2), pp.150–154.
- Fardeau, J.C., 1995. Dynamics of phosphate in soils. An isotopic outlook. *Fertilizer Research*, 45(2), pp.91–100.
- Fischer, R. & Lortenz, M., 2011. *Forest Condition in Europe 2011 Technical Report of ICP Forests and FutMon*, Hamburg.
- Flato, G. et al., 2013. Evaluation of Climate Models. In T. F. Stocker et al., eds. *Climate Change 2013: The Physical Science Basis*. Cambridge, United Kingdom and New York, NY, USA: Cambridge University Press, pp. 741–866.
- Fletcher, T.D., 2015. Package “QuantPsyc.”, p.26.
- Flückiger, W. & Braun, S., 1999. Nitrogen and its effect on growth, nutrient status and parasite attacks in beech and Norway spruce. *Water, Air, and Soil Pollution*, 116(1–2), pp.99–110.
- Fontes, L. et al., 2010. Models for supporting forest management in a changing environment. *Forest Systems*, 19, pp.8–29.
- Fowler, D. et al., 2013. The global nitrogen cycle in the twenty-first century. *Philosophical Transactions of the Royal Society B*, 368, p.20130164.
- Fox, T., Miller, B. & Rubilar, R., 2011. Phosphorus nutrition of forest plantations: The role of inorganic and organic phosphorus. In E. Bünemann, A. Oberson, & E. Frossard, eds. *Phosphorus in Action Biological Processes in Soil Phosphorus Cycling*. Berlin, Heidelberg: Springer Berlin Heidelberg, pp. 317–338.
- Frossard, E. et al., 2011. The Use of Tracers to Investigate Phosphate Cycling in Soil – Plant Systems. In E. Bünemann, A. Oberson, & E. Frossard, eds. *Phosphorus in Action Biological Processes in Soil Phosphorus Cycling*. Soil Biology. Berlin, Heidelberg: Springer Berlin Heidelberg, pp. 59–91.
- Frossard, E. & Sinaj, S., 1997. The Isotope Exchange Kinetic Technique: A Method to Describe the Availability of Inorganic Nutrients. Applications to K, P, S and Zn. *Isotopes in Environmental and Health Studies*, 34(1–2), pp.61–77.
- Goll, D.S. et al., 2012. Nutrient limitation reduces land carbon uptake in simulations with a model of combined carbon, nitrogen and phosphorus cycling. *Biogeosciences*, 9, pp.3547–3569.
- Gress, S.E. et al., 2007. Nutrient Limitation in Soils Exhibiting Differing Nitrogen Availabilities: What Lies Beyond Nitrogen Saturation? *Ecology*, 88(1), pp.119–130.
- Gundersen, P., Schmidt, I.K. & Raulund-Rasmussen, K., 2006. Leaching of nitrate from temperate forests — effects of air pollution and forest management. *Environmental Reviews*, 14, pp.1–57.
- Hinsinger, P. et al., 2011. Acquisition of phosphorus and other poorly mobile nutrients by roots . Where do plant nutrition models fail? *Plant and Soil*, 348, pp.29–61.
- Hinsinger, P., 2001. Bioavailability of soil inorganic P in the rhizosphere as effected by root-induced chemical changes: A review. *Plant and Soil*, 237, pp.173–195.
- Högborg, P. et al., 2006. Tree growth and soil acidification in response to 30 years of experimental nitrogen loading on boreal forest. *Global Change Biology*, 12(3), pp.489–499.
- Ingerslev, M. et al., 2001. Main Findings and Future Challenges in Forest Nutritional Research and Management in the Nordic Countries. *Scandinavian Journal of Forest Research*, 16, pp.488–501.
- Johnson, A.H., Frizano, J. & Vann, D.R., 2003. Biogeochemical Implications of Labile Phosphorus in Forest Soils

518 Determined by the Hedley Fractionation Procedure. *Oecologia*, 135(4), pp.487–499.

519 Jonard, M. et al., 2009. Forest floor contribution to phosphorus nutrition: experimental data. *Annals of Forest*
520 *Science*, 66(5), p.510p1-9.

521 Jonard, M. et al., 2010. Modeling forest floor contribution to phosphorus supply to maritime pine seedlings in two-
522 layered forest soils. *Ecological Modelling*, 221(6), pp.927–935.

523 Jonard, M. et al., 2015. Tree mineral nutrition is deteriorating in Europe. *Global Change Biology*, 21, pp.418–430.

524 Jones, D.L. & Oburger, E., 2011. Solubilization of Phosphorus by Soil Microorganisms. In E. Bünemann, A.
525 Oberson, & E. Frossard, eds. *Phosphorus in Action Biological Processes in Soil Phosphorus Cycling*. Berlin,
526 Heidelberg: Springer Berlin Heidelberg, pp. 169–198.

527 Kreutzer, K. et al., 2009. The complete nitrogen cycle of an N-saturated spruce forest ecosystem. *Plant Biology*,
528 11(5), pp.643–649.

529 Lang, F. et al., 2017. Soil phosphorus supply controls P nutrition strategies of beech forest ecosystems in Central
530 Europe. *Biogeochemistry*, 136(1), pp.5–29.

531 Likens, G.E., Driscoll, C.T. & Buso, D.C., 1996. Long-Term Effects of Acid Rain: Response and Recovery of a
532 Forest Ecosystem. *Science*, 272(5259), pp.244–246.

533 Linder, S., 1995. Foliar analysis for detecting and correcting nutrient imbalances in Norway spruce. *Ecological*
534 *Bulletins*, 44(44), pp.178–190.

535 Lindström, G. & Gardelin, M., 1992. Modelling groundwater response to acidification, Report from the Swedish
536 integrated groundwater acidification project. In P. Sandén & P. Warfvinge, eds. *SMHI, Reports Hydrology*. pp.
537 33–36.

538 Majdi, H. & Rosengren-Brinck, U., 1994. Effects of ammonium sulphate application on the rhizosphere, fine-root
539 and needle chemistry in a *Picea abies* (L) Karst stand. *Plant and Soil*, 162(1), pp.71–80.

540 Manzoni, S. et al., 2010. Stoichiometric controls on carbon, nitrogen, and phosphorus dynamics in decomposing
541 litter. *Ecological Monographs*, 80(1), pp.89–106.

542 Manzoni, S. & Porporato, A., 2009. Soil carbon and nitrogen mineralization: Theory and models across scales. *Soil*
543 *Biology and Biochemistry*, 41(7), pp.1355–1379.

544 McGechan, M.B. & Lewis, D.R., 2002. Sorption of Phosphorus by Soil, Part 1: Principles, Equations and Models.
545 *Biosystems Engineering*, 82(1), pp.1–24.

546 McGill, W.B. & Cole, C. V., 1981. Comparative aspects of cycling of organic C, N, S and P through soil organic
547 matter. *Geoderma*, 26(4), pp.267–286.

548 Mellert, K.H. & Göttelein, A., 2012. Comparison of new foliar nutrient thresholds derived from van den Burg's
549 literature compilation with established central European references. *European Journal of Forest Research*,
550 131(5), pp.1461–1472.

551 Messiga, A.J. et al., 2012. Process-based mass-balance modeling of soil phosphorus availability in a grassland
552 fertilized with N and P. *Nutrient Cycling in Agroecosystems*, 92(3), pp.273–287.

553 Moorhead, D.L. & Sinsabaugh, R.L., 2006. A theoretical model of litter decay and microbial interaction. *Ecological*
554 *Monographs*, 76(2), pp.151–174.

555 Morel, C. et al., 2014. Modeling of phosphorus dynamics in contrasting agroecosystems using long-term field
556 experiments. *Canadian Journal of Soil Science*, 94(3), pp.377–387.

557 Müller, C. & Bünemann, E.K., 2014. A 33P tracing model for quantifying gross P transformation rates in soil. *Soil*
558 *Biology and Biochemistry*, 76, pp.218–226.

559 Nelson, E. et al., 2011. The provisioning value of timber and non-timber forest products. In P. M. Kareiva et al., eds.
560 *Natural Capital: Theory and Practice of Mapping Ecosystem Services*. Oxford: Oxford University Press, pp.
561 129–149.

562 Newman, E., 1995. Phosphorus inputs to terrestrial ecosystems. *Journal of Ecology*, 83(4), pp.713–726.

Oberson, A. & Joner, E.J., 2005. Microbial Turnover of Phosphorus in Soil. In B. L. Turner, E. Frossard, & D. S. Baldwin, eds. *Organic Phosphorus in the Environment*. Wallingford: CABI, pp. 133–164.

Parton, W.J., Stewart, J.W.B. & Cole, C. V., 1988. Dynamics of C, N, P and S in grassland soils: a model. *Biogeochemistry*, 5(1), pp.109–131.

Reich, P.B. et al., 2006. Nitrogen limitation constrains sustainability of ecosystem response to CO₂. *Nature*, 440(7086), pp.922–925.

Rosengren-Brinck, U. & Nihlgård, B., 1995. Nutritional Status in Needles of Norway Spruce in Relation to Water and Nutrient Supply. *Ecological Bulletins*, 44, pp.168–177.

Rothpfeffer, C. & Karlton, E., 2007. Inorganic elements in tree compartments of *Picea abies*-Concentrations versus stem diameter in wood and bark and concentrations in needles and branches. *Biomass and Bioenergy*, 31(10), pp.717–725.

Runyan, C.W. & D’Odorico, P., 2012. Hydrologic controls on phosphorus dynamics: A modeling framework. *Advances in Water Resources*, 35, pp.94–109.

Santner, T.J., Williams, B. & Notz, W., 2003. *The Design and Analysis of Computer Experiments*, New York: Springer-Verlag.

Schimel, J.P. & Weintraub, M.N., 2003. The implications of exoenzyme activity on microbial carbon and nitrogen limitation in soil: A theoretical model. *Soil Biology and Biochemistry*, 35(4), pp.549–563.

Schoumans, O.F. & Groenendijk, P., 2000. Modeling soil phosphorus levels and phosphorus leaching from agricultural land in the Netherlands. *Journal of Environmental Quality*, 29, pp.111–116.

Shen, J. et al., 2011. Phosphorus Dynamics: From Soil to Plant. *Plant Physiology*, 156(3), pp.997–1005.

Simpson, D. et al., 2011. Atmospheric transport and deposition of reactive nitrogen in Europe. In M. A. Sutton et al., eds. *The European Nitrogen Assessment*. Cambridge: Cambridge University Press, pp. 298–316.

Smits, M.M. et al., 2012. Plant-driven weathering of apatite - the role of an ectomycorrhizal fungus. *Geobiology*, 10(5), pp.445–456.

Stroia, C., Morel, C. & Jouany, C., 2007. Dynamics of diffusive soil phosphorus in two grassland experiments determined both in field and laboratory conditions. *Agriculture, Ecosystems and Environment*, 119(1–2), pp.60–74.

Stroia, C., Morel, C. & Jouany, C., 2011. Nitrogen Fertilization Effects on Grassland Soil Acidification: Consequences on Diffusive Phosphorus Ions. *Soil Science Society of America Journal*, 75(1), pp.112–120.

Talkner, U. et al., 2015. Phosphorus nutrition of beech (*Fagus sylvatica* L.) is decreasing in Europe. *Annals of Forest Science*, 72(7), pp.919–928.

Tamm, C.O., 1991. *Nitrogen in Terrestrial Ecosystems* W. D. Billings et al., eds., Berlin: Springer-Verlag.

Tessier, J.T. & Raynal, D.J., 2003. Use of nitrogen to phosphorus ratios in plant tissue as an indicator of nutrient limitation and nitrogen saturation. *Journal of Applied Ecology*, 40(3), pp.523–534.

Tipping, E. et al., 2014. Atmospheric deposition of phosphorus to land and freshwater. *Environ. Sci.: Processes Impacts*, 16(7), pp.1608–1617.

Vestin, J.L.K. et al., 2013. The influence of alkaline and non-alkaline parent material on Norway spruce tree chemical composition and growth rate. *Plant and Soil*, 370(1–2), pp.103–113.

Wallander, H. & Thelin, G., 2008. The stimulating effect of apatite on ectomycorrhizal growth diminishes after PK fertilization. *Soil Biology and Biochemistry*, 40(10), pp.2517–2522.

Wallman, P. et al., 2006. DECOMP – a semi-mechanistic model of litter decomposition. *Environmental Modelling and Software*, 21(1), pp.33–44.

Wallman, P. et al., 2005. ForSAFE—an integrated process-oriented forest model for long-term sustainability assessments. *Forest Ecology and Management*, 207(1–2), pp.19–36.

- Walse, C., Berg, B. & Sverdrup, H., 1998. Review and synthesis of experimental data on organic matter decomposition with respect to the effect of temperature, moisture, and acidity. *Environmental Reviews*, 6(1), pp.25–40.
- Wang, Y.P., Houlton, B.Z. & Field, C.B., 2007. A model of biogeochemical cycles of carbon, nitrogen, and phosphorus including symbiotic nitrogen fixation and phosphatase production. *Global Biogeochemical Cycles*, 21(1), pp.1–15.
- Wang, Y.P., Law, R.M. & Pak, B., 2010. A global model of carbon, nitrogen and phosphorus cycles for the terrestrial biosphere. *Biogeosciences*, 7(7), pp.2261–2282.
- Werner, F. et al., 2017. Small-scale spatial distribution of phosphorus fractions in soils from silicate parent material with different degree of podzolization. *Geoderma*, 302(Supplement C), pp.52–65.
- Yanai, R.D., 1992. Phosphorus budget of a 70-year old northern hardwood forest. *Biogeochemistry*, 17, pp.1–22.
- Yanai, R.D., 1998. The effect of whole-tree harvest on phosphorus cycling in a northern hardwood forest. *Forest Ecology and Management*, 104(1–3), pp.281–295.
- Yang, X. et al., 2014. The role of phosphorus dynamics in tropical forests - A modeling study using CLM-CNP. *Biogeosciences*, 11(6), pp.1667–1681.
- Yang, X. & Post, W.M., 2011. Phosphorus transformations as a function of pedogenesis: A synthesis of soil phosphorus data using Hedley fractionation method. *Biogeosciences*, 8(10), pp.2907–2916.
- Yu, L. et al., 2016. Storm disturbances in a Swedish forest-A case study comparing monitoring and modelling. *Ecological Modelling*, 320, pp.102–113.
- Zanchi, G. et al., 2016. A Hydrological Concept including Lateral Water Flow Compatible with the Biogeochemical Model ForSAFE. *Hydrology*, 3(1), p.11.
- Zanchi, G. et al., 2014. Modelling the effects of management intensification on multiple forest services: a Swedish case study. *Ecological Modelling*, 284, pp.48–59.

Notations	Definitions	Location
<i>ActEvap</i> and <i>PotEvap</i>	actual and potential evapotranspiration rates, $\text{m}^3 \text{ water m}^{-2} \text{ soil d}^{-1}$	Eq. A1.1
<i>Perco</i>	percolation rate, $\text{m}^3 \text{ water m}^{-2} \text{ soil d}^{-1}$	Eq. A1.2
<i>Bypass</i>	bypass flow rate, $\text{m}^3 \text{ water m}^{-2} \text{ soil d}^{-1}$	Eq. A1.3
<i>Surface</i>	surface flow rate, $\text{m}^3 \text{ water m}^{-2} \text{ soil d}^{-1}$	Eq. A1.4
<i>moist</i>	soil moisture, $\text{m}^3 \text{ water m}^{-3} \text{ soil}$	Eq. A1.5
<i>wp</i>	wilting point of the soil, $\text{m}^3 \text{ water m}^{-3} \text{ soil}$	Eq. A1.1
<i>lp</i>	limit point for evapotranspiration of the soil, $\text{m}^3 \text{ water m}^{-3} \text{ soil}$	Eq. A1.1
<i>fc</i>	field capacity of the soil, $\text{m}^3 \text{ water m}^{-3} \text{ soil}$	Eq. A1.2
<i>fs</i>	field saturation of the soil, $\text{m}^3 \text{ water m}^{-3} \text{ soil}$	Eq. A1.3
<i>Kh</i>	unsaturated conductivity, m water d^{-1}	Eq. A1.3
<i>A</i>	area of the soil column, m^2	Eq. A1.3
<i>prec</i>	precipitation, m	Eq. A1.4
<i>z</i>	depth of the soil layer, m	Eq. A1.4
<i>t</i>	time step, d	Eq. A1.5
<i>C_{loss}</i>	mass loss rates of the decomposable compounds, $\text{g C m}^{-3} \text{ d}^{-1}$	Eq. A2.1
<i>k_{pot}</i>	potential mass loss rate constant at assumed optimal conditions, $\text{g C m}^{-3} \text{ d}^{-1}$	Eq. A2.1
<i>M</i>	mass of organic C of the decomposable compounds, g C	Eq. A2.1
<i>θ</i>	relative soil moisture, $\text{m}^3 \text{ water m}^{-3} \text{ water}$	Eq. A2.2
<i>T</i>	soil temperature, K	Eq. A2.3
<i>pH</i>	soil water pH	Eq. A2.5
<i>E_a</i>	activation energy, J mol^{-1}	Eq. A2.3
<i>R</i>	gas constant, $\text{J mol}^{-1} \text{ K}^{-1}$	Eq. A2.3
<i>T_r</i>	reference temperature, K	Eq. A2.3
<i>K_w</i>	empirical coefficient of moisture responding factor	Eq. A2.4
<i>n_w</i>	empirical exponent of moisture responding factor	Eq. A2.4
<i>K_{pH}</i>	response coefficient of acidity responding factor	Eq. A2.5
<i>m</i>	empirical exponent of acidity responding factor	Eq. A2.5
<i>DEC</i>	decomposition rate, $\text{g C m}^{-3} \text{ d}^{-1}$	Eq. A2.6
<i>η</i>	fraction of microbial assimilation in decomposition	Eq. A2.6
<i>k_{hum}</i>	fraction of stabilization (humification) in decomposition	Eq. A2.6
<i>k_{lch}</i>	fraction of DOC loss in decomposition	Eq. A2.6
<i>r_{min}</i>	mineralization rate, $\text{mg N(P) m}^{-3} \text{ d}^{-1}$	Eq. A2.7
<i>r_{blmin}</i>	biological mineralization rate, $\text{mg N(P) m}^{-3} \text{ d}^{-1}$	Eq. A2.8

r_{bcmin}	biochemical mineralization rate, mg $P\ m^{-3}\ d^{-1}$	Eq. A2.7
r_{OMmin}	mineralization rate, mg $N(P)\ m^{-3}\ d^{-1}$	Eq. A2.7
CPr	C: P ratios of the decomposable compounds	Eq. A2.8
CPr_{mic}	C: P ratios of the microbial biomass	Eq. A2.8
$MaxP_{bcmin}$	maximum potential P biochemical mineralization rate, mg $P\ m^{-3}\ d^{-1}$	Eq. A2.9
Mic	microbial biomass, g $C\ m^{-3}$	Eq. A2.9
P_o	sum of organic P in <i>holo</i> , <i>lig</i> and <i>recal</i> , mg $P\ m^{-3}\ soil$	Eq. A2.9
Cp	concentration of the dissolved inorganic phosphorous, mg $P\ dm^{-3}\ water$	Eq. A2.9
k_{enz}	maximum rate of enzymatic mineralization, $m^3\ g^{-1}\ C\ d^{-1}$	Eq. A2.9
P_{und}	unfulfilled P demand, mg $P\ m^{-3}\ d^{-1}$	Eq. A2.10
Mic_{OM}	microbial overflow metabolism C loss, g $C\ d^{-1}$	Eq. A2.11
Mic_{red}	microbial growth reduction due to nutrient limitation, g $C\ d^{-1}$	Eq. A2.11
Mic_{ass}	microbial assimilation, g $C\ d^{-1}$	Eq. A2.12
Mic_{resp}	microbial respiration, g $C\ d^{-1}$	Eq. A2.13
Mic_{decay}	microbial decay, g $C\ d^{-1}$	Eq. A2.14
f_{resp}	respiration rate of microbial biomass, d^{-1}	Eq. A2.13
f_{micdec}	decay rate coefficient of microbial biomass, d^{-1}	Eq. A2.14
r_{des}	desorption rate of P, mg $P\ m^{-3}\ d^{-1}$	Eq. A4.1
Pr_{tot0} and Pr_{tot}	total sorbed P in the soil matrix before and after the time step, mg $P\ kg^{-1}\ soil$	Eq. A4.1
Pr_{1d}	sorption capacity of the soil layer within one day, mg $P\ kg^{-1}\ soil$	Eq. A4.1
P_{bal}	total change rate of certain processes shown in Eq. B4.2, mg $P\ m^{-3}\ d^{-1}$	Eq. A4.2
r_{upt}	actual plant uptake of P, mg $P\ m^{-3}\ d^{-1}$	Eq. A4.2
r_{wea}	mineral weathering rate of P, mg $P\ m^{-3}\ d^{-1}$	Eq. A4.2
r_{dep} and r_{fert}	P deposition rate and fertilization rate, mg $P\ m^{-3}\ d^{-1}$	Eq. A4.2
v, w and x	fitted parameters from the isotopic dilution sorption experiments	Eq. A4.3, 4
T_{1yr} and T_{1d}	time in minutes for one year and one day	Eq. A4.3, 4
Cp_{eq}	equilibrium Cp at the soil solution and soil matrix interface, mg $P\ dm^{-3}\ water$	Eq. A4.3, 4
$Clay$	soil particles smaller than 2 μm , g kg^{-1}	Eq. A4.5
$Silt$	soil particles between 2 μm and 50 μm , g kg^{-1}	Eq. A4.6
$Sand$	soil particles between 50 μm and 2000 μm , g kg^{-1}	Eq. A4.5
P_{tot}	total P in the soil layer, g $P\ kg^{-1}\ soil$	Eq. A4.6
N_{org}	organic N in the soil layer, g $N\ kg^{-1}\ soil$	Eq. A4.7
$MaxPr_{tot}$	maximum soil P sorption capacity, mg $P\ m^{-3}$	Eq. A4.8
$(Al+Fe)_{ox}$	oxalate-extractable Al and Fe, mmol kg^{-1}	Eq. A4.8
mw_P	molecular weight of P, mg $mmol^{-1}$	Eq. A4.8

Q_{in} and Q	discharges of inflow and outflow of the soil layer, $\text{dm}^3 \text{ water m}^{-3} \text{ soil d}^{-1}$	Eq. A4.9
Cp_{in}	Cp in the inflow, $\text{mg P dm}^{-3} \text{ water}$	Eq. A4.9

A1 Soil hydrology

The simulations of soil water contents and flows are based on the soil hydrology module of the *ForSAFE* model (Zanchi et al. 2016). The soil is represented by a soil column with several layers denoting the soil horizons. The water flows by percolation or surface flow. The percolation is determined by the hydraulic conductivity and constrained by the capacity to receive water in the next layer, but in the last layer, it is restricted by the base flow rate, assuming that the water cannot drain freely. Surface flow occurs above the uppermost layer if it becomes oversaturated due to high precipitation or if percolation stops when the layers below are saturated.

$$ActEvap = \min(1, \max(0, \frac{moist-wp}{lp-wp})) \times PotEvap \quad (A1.1)$$

$$Perco = (\min(\min(\max(0, (moist - fc) \times z + Vol_{in} - ActEvap), Kh \times A \times t), \max(0, (fs_{next} - moist_{next}) \times z_{next}))) / t \quad (A1.2)$$

$$Bypass = (\min((moist - fc) \times z + Water_{in} - ActEvap, \max(0, (fs_{next} - moist_{next}) \times z_{next} + Kh_{next} \times A \times t))) / t \quad (A1.3)$$

$$Surface = (\max(0, moist_1 \times z_1 + prec_{in} - Perco_1 - Evap_1 - Bypass_1)) / t \quad (A1.4)$$

$$\theta = \theta_0 + Vol_{in} - ActEvap - (Perco - Bypass - Surface) \times t \quad (A1.5)$$

where *ActEvap* and *PotEvap* are the actual and potential evapotranspiration rates ($\text{m}^3 \text{ water m}^{-2} \text{ soil d}^{-1}$); *Perco*, *Bypass* and *Surface* are percolation, bypass flow and surface flow, respectively ($\text{m}^3 \text{ water m}^{-2} \text{ soil d}^{-1}$); θ is the soil moisture ($\text{m}^3 \text{ water m}^{-3} \text{ soil}$); *wp*, *lp*, *fc* and *fs* are the wilting point, limit point for evapotranspiration, field capacity and field saturation point of the soil, all in the unit $\text{m}^3 \text{ water m}^{-3} \text{ soil}$; *Vol_{in}* is the inflow water ($\text{m}^3 \text{ water}$), including percolation and bypass flow; *Kh* is the unsaturated conductivity (m water d^{-1}); *prec* is the precipitation (m), including melting snow; *z* is the depth of the soil layer (m); *A* is the area of the soil column (m^2); and *t* is the time step (d). The denotation *next* indicates the next layer; *1* indicates the first layer; and *0* indicates the value from the last time step.

The hydraulic properties (*wp*, *lp*, *fc*, *fs* and *Kh*) are estimated based on the soil input data, following the algorithms used in the work of Zanchi et al. (2016).

A2 Decomposition

In *ForSAFE*, SOM refers to the solid humified compounds in the soil and contains organic C, N and P. Following the concept of the *DECOMP* model (Walse et al. 1998), SOM is divided into four categories of decomposable compounds: *easily decomposable compounds (EDC)*, *holocellulose (holo)*, *lignin (lig)* and *recalcitrant compounds (recal)*. SOM is fed by fresh plant litter and newly decayed microbial biomass (Figure 2- Decomposition). It is assumed that plant litter contains *EDC*, *holo* and *lig*, whereas microbial necromass contains only *EDC* and *holo*. The description and distribution of compounds are given in SI.

The carbon loss rate of the decomposable compound is calculated as:

$$C_{loss_i} = k_{pot_i} M_i f_i(T) g_i(\theta) \phi_i(pH) \quad (A2.1)$$

$$\theta = moist / fs \quad (A2.2)$$

where C_{loss} is the carbon loss rate ($\text{g carbon m}^{-3} \text{ d}^{-1}$), *i* denotes the compound index (*EDC*, *holo*, *lig* or *recal*), k_{pot} is the potential rate constant at assumed optimal conditions ($\text{g carbon m}^{-3} \text{ d}^{-1}$), *M* is the mass of organic C of the decomposable compound (g carbon), *T* is the temperature of the soil layer (K), θ is the relative soil moisture, and *pH* is the soil water pH. The rate regulating functions are adopted from Walse et al. (1998),

$$f(T) = \exp\left(\frac{E_a}{R \cdot T_r} - \frac{E_a}{R \cdot T}\right) \quad (A2.3)$$

$$g(\theta) = \frac{K_w \cdot \theta^{n_w}}{1 + K_w \cdot \theta^{n_w}} \quad (A2.4)$$

$$\phi(pH) = \frac{1}{1 + K_{pH} \cdot [H^+]^m} \quad (A2.5)$$

where E_a is the activation energy (J mol⁻¹), R is the gas constant (J mol⁻¹ K⁻¹), T_r is the reference temperature (K), K_w is the empirical coefficient, n_w is the empirical exponent, K_{pH} is the response coefficient, and m is the empirical exponent. Values of the parameters are given in *ForSAFE parameterization*.

The decomposition rate of the decomposable compounds (total carbon loss of the compound category, DEC , g C m⁻³ d⁻¹) is calculated based on the mass loss rate:

$$DEC_i = \frac{C_{loss_i}}{(1 - \eta_i)(1 - k_{hum_i} - k_{lch_i})} \quad (A2.6)$$

where i denotes the compound category; η is the assimilation factor that represents the fraction of DEC assimilated by microbes for growth; k_{hum} is the humification coefficient, which represents the fraction of DEC that forms recalcitrant compounds; and k_{lch} is the leaching coefficient, which represents the fraction of DEC that forms dissolved organic carbon (DOC) (Berg & McClaugherty 2008).

Soil organic nutrients are associated with the decomposition of C and therefore are humified to form recalcitrant compounds, enter the soil solution in dissolved inorganic forms (mineralization), or are assimilated by microbes (immobilization) (Figure 2- Decomposition). The mineralization rate (r_{min} , mg m⁻³ d⁻¹) can be divided into biological mineralization (r_{blmin} , mg m⁻³ d⁻¹), biochemical mineralization (r_{bcmin} , mg m⁻³ d⁻¹, only P) and overflow metabolism mineralization (r_{OMmin} , mg m⁻³ d⁻¹):

$$r_{min} = r_{blmin} + r_{bcmin} + r_{OMmin} \quad (A2.7)$$

$$r_{blmin} = \sum_{i=1}^n DEC_i \left(\frac{1 - k_{hum_i}}{CPr_i} - \frac{(1 - k_{hum_i} - k_{lch_i})\eta_i}{CPr_{mic}} \right) \quad (A2.8)$$

where CPr and CPr_{mic} are the C: P ratios of the compounds and microbial biomass, respectively; for N CNr and CNr_{mic} are used in Eq. B2.8.

Apart from biological mineralization, the nutrients in organic forms can also become plant available through C overflow metabolism and biochemical mineralization. Carbon overflow metabolism is the elimination of C and nutrients from microbial biomass when C is in excess (Schimel & Weintraub 2003; Manzoni & Porporato 2009). It is treated in the same way as microbial decay, except that all the overflowed C is respired. Biochemical mineralization (r_{bcmin} , mg m⁻³ d⁻¹, mineralization catalyzed by enzymes and without releasing CO₂, McGill & Cole 1981; Oberson & Joner 2005) accounts only for P, and the rate is as follows:

$$MaxP_{bcmin} = \begin{cases} Mic \cdot P_o \cdot k_{enz} \cdot f(T, \theta, pH) & \text{if } Cp \leq 0.005 \\ Mic \cdot P_o \cdot k_{enz} \cdot \frac{Cp^{-0.5}}{0.005^{-0.5}} \cdot f(T, \theta, pH) & \text{if } Cp \geq 0.005 \end{cases} \quad (A2.9)$$

$$r_{bcmin} = \min(MaxP_{bcmin}, P_{und}) \quad (A2.10)$$

where P_{org} is the sum of organic P in *holo*, *lig* and *recal* (mg P m⁻³); $MaxP_{bcmin}$ is the maximum potential P biochemical mineralization rate (mg P m⁻³ d⁻¹); Cp is the concentration of dissolved inorganic phosphorous (mg P dm⁻³ water); k_{enz} is the maximum rate of enzymatic mineralization (m³ g⁻¹ C d⁻¹); $f(T, \theta, pH)$ is the rate response function given in Eq. B.3, B.4 and B.5; and P_{und} is the unfulfilled P demand (mg P m⁻³ d⁻¹). It is assumed that the maximum biochemical mineralization rate is higher when Cp is low, and it has a maximum rate when the threshold concentration for plant uptake (0.005 mg P dm⁻³ water, Stroia et al. 2007) is reached.

Microbes are heterotrophic decomposers that form biomass from decomposed C and nutrients. Microbes are the sole decomposer in the model. The following assumptions are made: first, the carbon-to-nutrient ratios of new microbial biomass are strictly restricted within certain ranges (Cleveland & Liptzin 2007; Parton et al. 1988; Manzoni et al. 2010); second, the microbial biomass decays at a certain rate (f_{micdec}), and the decayed microbial biomass (microbial necromass) is assumed to be *EDC* and *holo* and will be decomposed again. The change in microbial biomass is described as:

$$\frac{dMic}{dt} = Mic_{ass} - Mic_{resp} - Mic_{OM} - Mic_{red} - Mic_{decay} \quad (A2.11)$$

$$Mic_{ass} = \sum_{i=1}^n DEC_i (1 - k_{hum_i} - k_{lch_i}) \eta_i \quad (A2.12)$$

$$Mic_{resp} = Mic \cdot f_{micresp} \quad (A2.13)$$

$$Mic_{decay} = Mic \cdot f_{micdec} \quad (A2.14)$$

where Mic_{ass} is the microbial assimilation (g C d⁻¹); Mic_{resp} is the microbial respiration (g C d⁻¹); Mic_{OM} is the

microbial overflow metabolism C loss (g C d^{-1}); Mic_{red} is the microbial growth reduction due to nutrient limitation (g C d^{-1}); Mic_{decay} is the microbial decay (g C d^{-1}); $f_{micresp}$ is the maintenance respiration rate of microbial biomass (d^{-1}); and f_{micdec} is the decay rate coefficient of microbial biomass (d^{-1}). The Mic_{OM} and Mic_{red} occur at nutrient deficiency, and they are dependent on the amount of nutrient deficient and the carbon-to-nutrient ratios of microbial biomass.

A3 Tree growth

Two main changes have been introduced to the tree structure: first, P has been added as a macro nutrient in plants, and second, a new compartment for twigs is distinguished from wood. Changes have also been made regarding plant uptake and nutrient allocation. The potential plant uptake is calculated as the growth rate of each tree compartment times the optimal nutrient content of the tree compartment during growing season of foliage and wood, and it is calculated as 110% of the root nutrient demand in non-growing season. The timing of nutrient uptake for foliage growth has been changed from only once per year at bud burst to multiple times synchronous with foliage growth. The wood growth has been changed from being limited only by plant C pool to being limited by both the C and nutrient pools in plant.

Four mechanisms have been introduced to regulate the N and P uptake of plants and microbes, namely plant uptake downscaling, microbial immobilization downscaling, microbial overflow metabolism and biochemical mineralization. When the nutrient demands (plant uptake and microbial immobilization) exceed nutrient availability, plant uptake and growth will first be decreased, followed by a reduction in microbial growth to reduce immobilization, and finally a reduction in microbial biomass by eliminating some carbon and nutrients. Biochemical mineralization accounts only for P and is negatively related to C_p .

A4 Soil inorganic P cycle

In ForSAFE, the P deposition (r_{dep} , $\text{mg P m}^{-3} \text{d}^{-1}$) is treated as model input and the weathering of P (r_{wea} , $\text{mg P m}^{-3} \text{d}^{-1}$) is simulated by the soil chemistry module, SAFE (Belyazid 2006).

The sorption/desorption process of P refers to all the inorganic P ion exchange processes (except weathering) between the soil solution and soil matrix. The desorption rate (P ions moving from the soil matrix to soil solution, r_{des} , $\text{mg P m}^{-3} \text{d}^{-1}$) is modeled as the change of total sorbed Pi in the soil matrix between two time steps (Stroia et al. 2007; Messiga et al. 2012; Morel et al. 2014). It is then constrained by the sorption capacity of the soil layer within the time step (Pr_{Id} , $\text{mg P m}^{-3} \text{soil}$):

$$r_{des} = \begin{cases} Pr_{tot0} - Pr_{tot}, & -Pr_{1d} < P_{bal} < Pr_{1d} & (a) \\ -Pr_{1d}, & P_{bal} < -Pr_{1d} < 0 & (b) \\ Pr_{1d}, & P_{bal} \geq Pr_{1d} \geq 0 & (c) \end{cases} \quad (\text{A4.1})$$

where Pr_{tot0} and Pr_{tot} are the total sorbed P in the soil matrix ($\text{mg P kg}^{-1} \text{soil}$) before and after the time step, and P_{bal} is the total change rate of all the other processes ($\text{mg P m}^{-3} \text{d}^{-1}$) that exert a direct impact on C_p (fertilization, deposition, weathering, plant uptake and immobilization/mineralization) and is given by

$$P_{bal} = r_{fert} + r_{dep} + r_{wea} + r_{min} + r_{upt} \quad (\text{A4.2})$$

when P_{bal} does not exceed the range of Pr_{Id} , sorption equilibrium is reached (condition B4.1.a); otherwise maximum net sorption (condition B4.1.b) or maximum net desorption (condition B4.1.c) occurs.

According to Forssard & Sinaj (1997) and Fardeau (1996), the total desorbed P is calculated using the Freundlich kinetic equation, assuming that the exchangeable Pi between soil matrix and soil solution within a year is the total sorbed P in the soil matrix (Eq. B4.3). The sorption capacity of a time step (day) is defined as the exchangeable Pi within the time step (Eq. B4.4):

$$Pr_{tot} = vC_{peq}^w (T_{1yr})^x \quad (\text{A4.3})$$

$$Pr_{1d} = vC_{peq}^w (T_{1d})^x \quad (\text{A4.4})$$

where v , w and x are fitted parameters from the isotopic dilution sorption experiments, with their estimation given in ForSAFE parameterization; T_{1yr} is the time in minutes and, for Eq. D.3, equals $24*60*365$; T_{1d} is the time in minutes and, for Eq. D.4, equals $24*60$; and C_{peq} is the equilibrium C_p at the soil solution and soil matrix interface ($\text{mg P dm}^{-3} \text{water}$). Note here that the total sorbed Pi and daily sorption capacity are related to the equilibrium C_p .

The parameters (v , w , and x) in the Freundlich kinetic equation are determined through isotopic dilution experiments (Stroia et al. 2007). *ForSAFE* also offers pedotransfer functions (Eq. B4.5 – B4.7) to estimate the parameters based on the physical-chemical properties of the soils from selected studies (Stroia et al. 2007; Achat et al. 2010; Morel et al. 2014; Stroia et al. 2011; Messiga et al. 2012).

$$v = 74.84 \times Clay + 9.40 \times Sand - 0.099 \times Fe_{ox} + 0.032 \times Al_{ox} + 1.04 \times pH + 1.12 \times P_{tot} - 14.29 \quad (A4.5)$$

$$w = 0.34 \times Silt - 1.089 \times Clay - 0.045 \times pH - 0.11 \times P_{tot} + 0.99 \quad (A4.6)$$

$$x = 0.11 \times Clay + 0.023 \times N_{org} + 0.26 \quad (A4.7)$$

where *Clay* ($g\ kg^{-1}$) is soil particles smaller than 2 μm ; *Silt* ($g\ kg^{-1}$) is soil particles between 2 and 50 μm ; *Sand* ($g\ kg^{-1}$) is soil particles between 50 and 2000 μm ; P_{tot} is the total phosphorus in the soil layer ($g\ P\ kg^{-1}\ soil$); and N_{org} is the organic nitrogen of the soil layer ($g\ N\ kg^{-1}\ soil$).

There is a maximum soil P sorption capacity ($MaxPr_{tot}$, $mg\ P\ kg^{-1}\ soil$) in the model that is assumed to be related to the sum of oxalate-extractable Al and Fe ($(Al+Fe)_{ox}$, $mmol\ kg^{-1}\ soil$) (Schoumans & Groenendijk 2000):

$$MaxPr_{tot} \approx 0.5 (Al + Fe)_{ox} \cdot mw_P \quad (A4.8)$$

where mw_P is the molecular weight of P ($mg\ mmol^{-1}$).

The C_p in *ForSAFE* is solved using the following equation:

$$\frac{\partial C_p}{\partial t} \cdot moist = Q_{in} \cdot Cp_{in} - Cp \left(Q + \frac{\partial moist}{\partial t} \right) + r_{des} + r_{wea} + r_{dep} + r_{min} + r_{upt} \quad (A4.9)$$

where Q_{in} and Q are the discharges of inflow and outflow of the soil layer, respectively ($dm^3\ water\ m^{-3}\ soil\ d^{-1}$);

Cp_{in} is the concentration of dissolved Pi in the inflow ($mg\ P\ dm^{-3}\ water$).